RSC Advances

ROYAL SOCIETY OF CHEMISTRY

www.rsc.org/advances

Journal Name

ARTICLE

Protein-surfactant aggregate as potential corrosion inhibitor for mild steel in sulphuric acid: Zein-SDS system

Pialee Roy, Dipankar Sukul*

The corrosion inhibition of mild steel in 0.5 M H_2SO_4 in presence of Zein (a biocompatible water insoluble corn protein) and sodium dodecyl sulfate (SDS, an anionic surfactant) is studied employing electrochemical techniques and gravimetric measurement. SEM and FTIR techniques are employed to observe the morphology of corroded surface and nature of the adsorbed layer. It is revealed that SDS micelles in high concentration exhibit low corrosion inhibition efficiency for mild steel in H_2SO_4. But inhibition efficiency increases drastically in Zein-SDS mixed system, reaching more than 90% in presence of 4 mM SDS-500 ppm Zein. Dependence of inhibition efficiency on surfactant-protein ratio is explained by Zein-SDS complex formation, followed by SDS induced conformational change of Zein.

Introduction

Corrosion inhibition of metals and alloys by the suitable inorganic and organic inhibitors has been the focus of research for decades. In recent years, research on biocompatible green corrosion inhibitor has taken tremendous impetus primarily due to environmental concern. Different biomolecules have now been tested for their potential anticorrosive properties towards various metals and alloys and in different corrosive environments.[1-14] Presence of heteroatoms like S, N, O, as well as aromatic groups and large molecular volume makes the biomolecules suitable to act as good corrosion inhibitor. In this paper, corrosion inhibition properties of one of the most important industrial corn protein, Zein, in combination with anionic surfactant, sodium dodecyl sulphate (SDS) have been assessed for mild steel in 0.5 M H_2SO_4. Zein is long been known for its use in fields like textile, cosmetics, paints, medicines, etc.[15,16] Large amount of hydrophobic residues in Zein, such as leucine (20%), proline (9%), alanine (14%), and glutamine (20%) make it almost

Department of Chemistry, National Institute of Technology, Durgapur, West Bengal, 713209, India. E-mail: dipankar.sukul@gmail.com; Tel: +91 9434788066

insoluble in aqueous solution.[17] In acidic condition, Zein is reported to carry positive charges, possibly due to the high glutamine residue exposure in its tertiary structure.[18] Its solubility in water increases many fold in presence of anionic surfactant SDS, which provides the dielectric constant of the aqueous surfactant solution comparable to water-alcohol mixture.[19,20] Anionic SDS, on the other hand, has versatile applications including as corrosion inhibitor.[21,22] Above critical micellar concentration (CMC), it forms spherical micelles in aqueous solution, having anionic head groups protruding outwards, while the aliphatic chains forming the hydrophobic core.[23]

In this paper, we have focused on the effect of polymer-surfactant interaction between Zein and SDS, which is supposed to initiate by electrostatic interaction (between net positive charge of Zein and negatively charged head groups of SDS), following by polymer-surfactant complex formation[19,20], towards their adsorption on mild steel surface in acidic media, and subsequent inhibition of corrosion of the metal. Different electrochemical techniques, like potentiodynamic polarization (Tafel extrapolation), electrochemical impedance spectroscopy (EIS), as well as gravimetric measurements have been employed for this purpose.

Experimental

Metal coupons preparation and chemicals

Test specimens were cut from a commercially available mild steel rod (wt% composition: 0.24 C, 0.40 Si, 0.90 Mn, 0.07 Ni, 0.03 Cr, 0.01 P, 0.005 S and the remainder iron). The cross-sectional surface was ground with different grade emery papers (400, 600, 800, 1200 and 1600), washed with water and acetone, and used as the working electrode in electrochemical measurements. SDS (Sigma-Aldrich) and Zein (Sigma) were used without any further purification. As molecular weight of Zein could not be determined accurately for its inherent molecular complexity, concentration of Zein was expressed in terms of ppm by weight.

Electrochemical measurements

Potentiodynamic polarization and electrochemical impedance measurement were done by conventional three-electrode system (model: Gill AC, ACM Instruments, UK) consisting of mild steel working electrode (WE) with an exposed area of 0.25 cm^2, platinum as counter electrode and saturated calomel electrode (SCE) as reference. Before electrochemical tests, the WE was kept in the test solution for sufficient time for attainment of steady open circuit potential (OCP). Polarization experiment was done for the potential range of ± 250 mV from OCP with a potential sweep rate of 30 mV per min. Corrosion current density (i_{corr}) was determined from the intercept of extrapolated cathodic and anodic Tafel lines at the corrosion potential (E_{corr}). The values of inhibition efficiency, $\eta_P(\%)$ were calculated from the following equation:

$$\eta_P(\%) = \frac{i_{corr} - i_{corr(inh)}}{i_{corr}} \times 100 \tag{1}$$

where, i_{corr} and $i_{corr(inh)}$ are the values of corrosion current density of uninhibited and inhibited specimens, respectively.

Electrochemical impedance (EIS) measurements were performed in the frequency range 10 mHz to 100 kHz with a.c. amplitude of ± 10 mV (rms) at the rest potential. Nyquist plots obtained, showed only one time constant corresponding to one capacitive loop without any trace of inductive loop at low frequency range. These capacitive loops were depressed with centre under the real axis, which may correspond to the microscopic roughness of the electrode surface and inhibitor adsorption on it.[24-27] Accordingly, these were fitted using an equivalent circuit consisting of parallel combination of charge transfer resistance-constant phase element, which was in series with solution resistance, $R_s[R_{ct}\text{-}CPE]$.[24-27] The impedance of CPE is given by

$$Z_{CPE} = Q^{-1} (i\omega)^{-n} \tag{2}$$

where, Q is a proportionality coefficient, ω is the angular frequency, n is a measure of surface irregularity. Q is an indicative parameter proportional to the capacitance of the double layer formed at the metal surface for $0 > n > 1$. For whole numbers of n = 1, 0, -1 CPE is reduced to the classical lumped elements capacitor (C), resistance (R), and inductance (L), respectively. Goodness of the fit was assessed from chi-squared values, which were in the range 10^{-3} to 10^{-5}. To correlate the charge transfer resistance (R_{ct}) and the double layer capacitance (C_{dl}) among the metal-solution interface, the later had been recalculated using the equation[27,28]

$$C_{dl} = (Q.R_{ct}^{1-n})^{1/n} \tag{3}$$

The percentage inhibition efficiencies $\eta_Z(\%)$ in terms of R_{ct} were calculated through the following equation:

$$\eta_Z(\%) = \frac{R_{ct} - R_{ct}^0}{R_{ct}} \times 100 \tag{4}$$

All the experiments had been carried out at around the room temperature of 30°C.

Weight loss measurements

For weight loss measurement, polished, dried and accurately weighed rectangular mild steel coupons ($2.5 \times 2.5 \times 0.1$ cm^3) were immersed in 0.5 M H_2SO_4 without and with inhibitor for a duration of 6h at room temperature around 30°C. Then, these were removed from the acid solution, scrubbed with bristle brush, washed thoroughly with distilled water and acetone, dried in a vacuum desiccator, and weighed. Percentage inhibition efficiency, $\eta_W(\%)$ was calculated following the relation:

$$\eta_W(\%) = \frac{W_0 - W}{W_0} \times 100 \tag{5}$$

where, W_0 and W are the weight loss of the metal coupons in acid medium without and with inhibitor.

Surface analysis

Scanning electron microscope (SEM, S-3000N, Hitachi) was used to study the surface morphology of metal surface after immersion in 0.5 M H_2SO_4 without and with inhibitor for a duration of 6h. The surface of the dried specimen was scratched

with a knife and the resultant powder was used for FTIR studies (KBr pellet method, Thermo Nicolet, model iS10).

Results and discussion

Polarization measurements

The potentiodynamic polarization measurements are carried out to study the anodic and cathodic reactions occurring on mild steel electrode in 0.5 M H_2SO_4 solution with addition of various concentration of SDS, in absence and presence of different concentrations of Zein (Fig. 1 and 2). Corresponding values of electrochemical parameters, such as corrosion potential (E_{corr}), corrosion current density (i_{corr}), anodic and cathodic Tafel slopes (b_a and b_c), as well as corrosion inhibition efficiency, $\eta_P(\%)$, are listed in Table 1. It is observed that
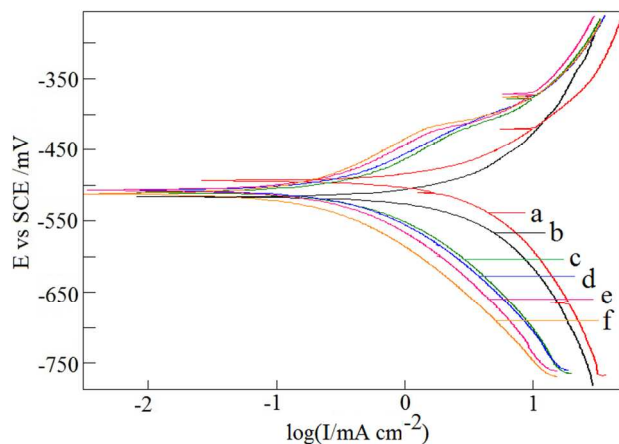
Fig. 1 Potentiodynamic polarization curves for mild steel in 0.5 M H_2SO_4 in presence of (a) no inhibitor, (b) 4 mM SDS, that with Zein having conc. (c) 50 ppm, (d) 100 ppm, (e) 250 ppm, (f) 500 ppm.
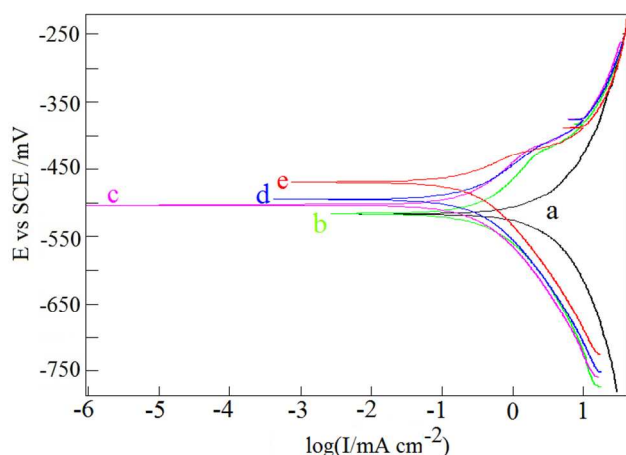
the nature of the potentiodynamic polarization curves for mild steel in 0.5 M H_2SO_4 solution in presence of SDS with concentration range 2 mM to 30 mM do not change to any reportable extent with respect to that of the blank solution. It may be mentioned here that critical micellar concentration (CMC) of SDS in 0.5 M H_2SO_4 solution is reported to be 0.8 mM,[29] and hence the concentration range of SDS used in the present study is much higher its CMC. Thus it may be concluded that SDS, at concentrations much higher than its CMC, cannot hinder the rate of either cathodic reduction (hydrogen evolution) or anodic reactions (metal dissolution) occurring at the cathodic and anodic reaction sites, respectively, on mild steel surface in H_2SO_4 solution to any appreciable extent.[30] It may be associated with the

tendency of SDS micelles to remain in the solution phase more than to get adsorbed on the metal surface.

Table 1 Data from potentiodynamic polarization studies for mild steel in 0.5 M H_2SO_4 in various inhibitor systems.

SDS (mM)	Zein (ppm)	$-E_{corr}$ (mV/ SCE)	i_{corr} (mA cm^{-2})	β_a (mV dec^{-1})	$-\beta_c$ (mV dec^{-1})	$\eta_P(\%)$
0	0	517	1.70	92.8	114.3	
2	0	498	1.44	80.6	104.5	15.3
	50	489	0.30	65.0	77.0	82.3
	100	514	0.28	76.0	94.6	83.5
	250	516	0.25	64.7	85.6	85.3
4	0	494	1.60	76.7	102.0	5.8
	50	510	0.33	75.6	101.5	80.5
	100	508	0.27	67.3	101.0	84.1
	250	503	0.20	65.4	104.2	88.2
	500	512	0.15	68.7	100.6	91.2
10	0	504	1.57	71.3	101.7	7.6
	50	504	0.37	65.7	101.0	78.2
	100	484	0.30	64.7	103.0	82.4
	250	495	0.22	67.5	101.0	87.0
	500	493	0.20	63.2	102.5	88.2
30	0	499	1.65	72.6	103.0	2.9
	50	497	0.41	65.4	100.0	75.9
	100	498	0.34	67.0	101.0	80.0
	250	469	0.32	57.7	93.8	81.2
	500	489	0.27	66.2	100.0	84.1

Significant change in potentiodynamic polarization curves is observed when Zein is added in the acidic SDS solution (Fig. 1 and 2; Table 1). Both the rate of cathodic and anodic reactions are clearly seen to decrease significantly with the E_{corr} values remaining very close to that of uninhibited sample. This indicates that when polymer-surfactant aggregate is formed and present on the mild steel surface, it acts as mixed type corrosion inhibitor. For a particular SDS concentration, i_{corr} values are seen to decrease gradually with increase in Zein concentration.

**Fig. 2** Potentiodynamic polarization curves for mild steel in 0.5 M H_2SO_4 in presence of (a) no inhibitor, 250 ppm Zein with SDS having conc. (b) 2 mM , (c) 4 mM, (d) 10 mM, (e) 30 mM.

It is worth mentioning that for a fixed Zein concentration in Zein-SDS aggregate, changes in inhibition efficiency shows a complex behaviour with increase in SDS concentration. For 50 ppm Zein, maximum inhibition efficiency is observed at 2 mM of SDS, thereafter it decreases slowly with SDS concentration. For higher concentration of Zein (100-500 ppm), maximum inhibition efficiency is seen around 4 mM SDS. Thus, corrosion inhibition effect of protein-surfactant complex displays dependence on protein-surfactant ratio. With gradual increase in SDS-Zein ratio, it is seen that the anodic polarization curves do not change significantly, but cathodic polarization curves get modified exhibiting increase in the rate of cathodic reduction reaction (Fig. 2). E_{corr} values also show gradual shift towards less negative direction. This indicates that after exhibiting maximum corrosion potentiality by Zein-SDS aggregate, if concentration of SDS is increased further, overall rate of corrosion tends to increase mostly due to enhancement in the rate of cathodic reduction reaction.[30]

Electrochemical impedance measurements

Nyquist plots, derived from EIS experiment, for mild steel in H_2SO_4 solution in presence of different concentrations of SDS and Zein-SDS complex with varied concentration ratio are shown in Fig. 3 and 4.
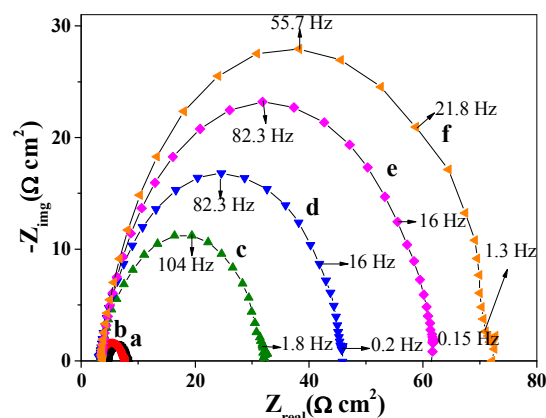
Fig. 3 Nyquist plots for mild steel in 0.5 M H_2SO_4 in presence of (a) no inhibitor, (b) 4 mM SDS, that with Zein having conc. (c) 50 ppm, (d) 100 ppm, (e) 250 ppm, (f) 500 ppm.

Fitting these plots using the equivalent circuit, as described in electrochemical measurements section, the corresponding fitting parameters and the inhibition efficiencies, η_Z(%) obtained from the R_{ct} values are tabulated in Table 2. It is observed that the diameter of the capacitive loops for mild steel in H_2SO_4 solution in presence of different concentrations of SDS are almost same with that of the blank solution. This indicates SDS at concentrations much higher than its CMC, cannot effectively cover the reaction sites on the metal surface, and therefore is unable to change the charge transfer resistance along the metal-solution interface.
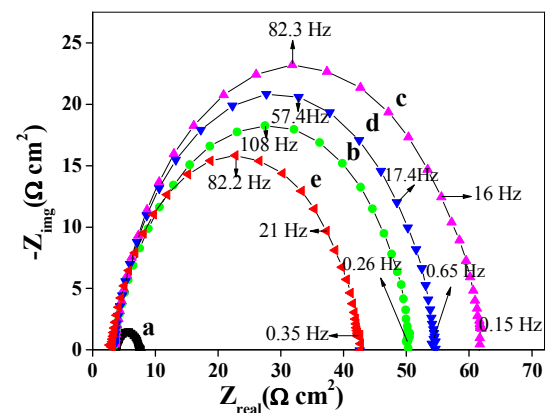
Fig. 4 Nyquist plots for mild steel in 0.5 M H_2SO_4 in presence of (a) no inhibitor, 250 ppm Zein with SDS having conc. (b) 2 mM , (c) 4 mM, (d) 10 mM, (e) 30 mM.

Table 2 Impedance parameters for the corrosion of mild steel in 0.5 M H$_2$SO$_4$ in various inhibitor systems.

SDS (mM)	Zein (ppm)	R_{ct} (Ω cm^2)	Q ($\mu\Omega^{-1}$s^n cm^{-2})	n	C_{dl} (μF cm^{-2})	η_Z(%)
0	0	3.7	740	0.82	203.0	
2	0	4.7	605	0.84	198.0	21.3
	50	30.0	155	0.83	51.6	87.6
	100	37.5	125	0.83	41.7	90.1
	250	47.0	95	0.84	33.9	92.1
4	0	4.2	623	0.83	184.0	11.9
	50	28.6	144	0.83	46.7	87.0
	100	42.6	120	0.84	43.9	91.3
	250	59.0	100	0.85	40.4	93.7
	500	68.6	89	0.86	38.8	94.6
10	0	4.3	600	0.83	177.0	13.9
	50	28.0	167	0.84	60.1	86.7
	100	34.0	138	0.84	49.7	89.1
	250	51.5	102	0.86	43.4	92.8
	500	64.8	83.4	0.87	38.2	94.3
30	0	4.0	686	0.85	24.2	7.5
	50	23.0	200	0.82	61.4	83.9
	100	29.3	146	0.85	55.7	87.3
	250	39.5	120	0.86	50.2	90.6
	500	52.0	102	0.87	46.6	92.8

Diameter of the capacitive loops, however, is seen to increase gradually with Zein concentration in acidic SDS micellar solution. Thus, it may be concluded that protein-surfactant aggregates efficiently adsorb on the mild steel surface in acidic media and

blocks the reaction sites on the metal surface, thereby increasing the charge transfer resistance and corrosion inhibition efficiency.[8-14,24-28] At higher SDS-Zein ratio, however, charge transfer resistance tends to decrease. This suggests to any possible structural change in Zein-SDS aggregate which compels the aggregate to desorb to some extent from the metal surface leaving the reaction sites easily accessible to corrosive environment.
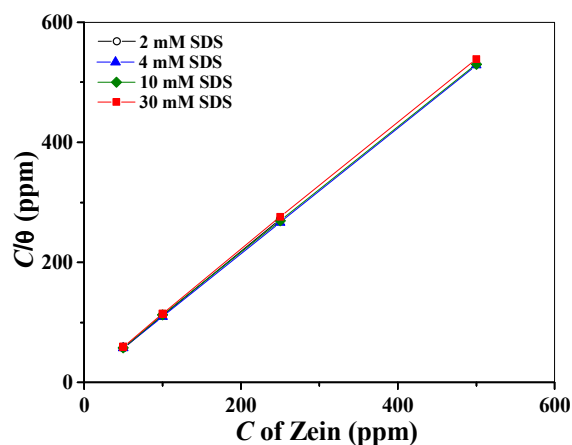
Adsorption isotherm

Langmuir adsorption isotherm model, which is based on the assumption that all the adsorption sites are energetically equivalent, has been applied towards the adsorption on Zein-SDS aggregate on the mild steel surface in H$_2$SO$_4$ solution. As per this model, degree of surface coverage θ ($\theta = \eta_Z$(%)/100) is related to the concentration of the inhibitor (C) following the relation:[31]

$$C/\theta = 1/K_{ads} + C \tag{6}$$

where, K_{ads} is constant of adsorption. As SDS itself does not show any appreciable corrosion inhibition in the present study, only the concentration of Zein present in different micellar solution is considered during fitting of the experimental data as per the above equation. Good linear fits (correlation coefficient, R^2 =0.999) are obtained for all the micellar solutions with slope values very close to 1 (Fig. 5). From the values of the adsorption constant, K_{ads}, the standard free energy of adsorption (ΔG^0_{ads}) for all the inhibitor systems are determined using the following equation:[28]

$$\Delta G^0_{ads} = -RT \ln(1 \times 10^6 K_{ads}) \tag{7}$$

where, 1×10^6 is the concentration of water molecules expressed in mg L^{-1}, R is the universal gas constant and T be the temperature (here, 303K) (Table 3). It is seen that in presence of higher concentration of SDS, K_{ads} for adsorption of Zein on mild steel in acid medium is lesser. As ΔG^0_{ads} value corresponds to an equilibrium state, based on this one cannot draw any definite conclusion whether adsorption takes place through physical (i.e., charge sharing between the inhibitor and metal) or chemical (i.e., complete charge transfer between the inhibitor molecule and metal) means. But, as a rough estimate and comparing the values given in literatures, it may be said that for present system with

Fig. 5 Langmuir adsorption plot for mild steel in 0.5 M H$_2$SO$_4$ in presence of different combinations of SDS and Zein.

ΔG^0_{ads} value of around -30 kJ mol^{-1}, physical adsorption (i.e. electrostatic interaction) is predominant over chemical adsorption.[10-14]

Table 3 Calculated parameters from Langmuir Adsorption Isotherm

Inhibitor system	Slope	R^2	K_{ads} (L mg^{-1})	ΔG^0_{ads} (kJ mol^{-1})
2 mM SDS and Zein	1.07	0.9999	2.77x10^{-1}	-31.5
4 mM SDS and Zein	1.04	1	2.0x10^{-1}	-30.7
10 mM SDS and Zein	1.04	0.9999	1.52x10^{-1}	-30.1
30 mM SDS and Zein	1.06	0.9999	1.27x10^{-1}	-29.6

Weight loss measurement

We have verified the results obtained from electrochemical measurements with gravimetric analysis. Variation of weight loss of mild steel in 0.5 M H$_2$SO$_4$ solution in presence of different concentrations of Zein (50 ppm to 500 ppm) together with various concentrations of SDS in the range 2 mM to 30 mM are shown in Fig. 6. It is seen the η_W(%)is always higher with higher concentration of Zein for all the concentrations of SDS used. It is also seen that with 50 ppm Zein, maximum η_W(%) is
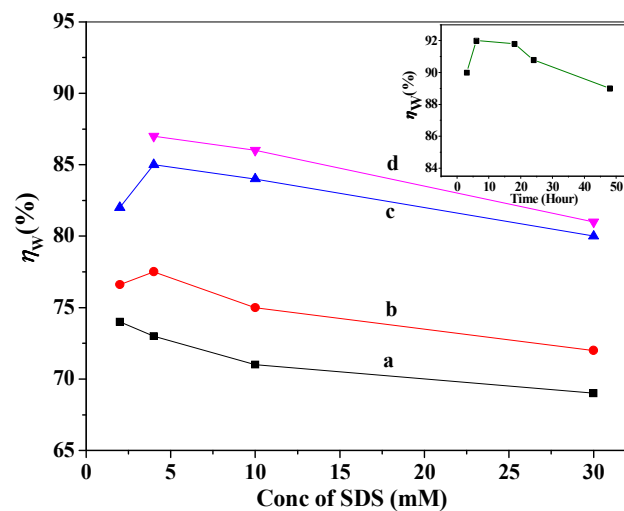

Fig. 6 Variation of inhibition efficiency of different concentrations of SDS (2mM to 30mM) with that of Zein having concentration (a) 50 ppm (b) 100 ppm (c) 250 ppm (d) 500 ppm. Figure in the inset shows variation of inhibition efficiency of 4mM SDS with 500 ppm Zein with immersion time.

obtained in the solution having 2 mM SDS and thereafter it declines slowly. While, for higher concentrations of Zein, solution with 4 mM SDS provides maximum η_W(%). Thus it is confirmed that surfactant-protein ratio plays some important role for the adsorption of protein-surfactant complex on mild steel and its subsequent corrosion inhibition in acid medium. From the observed variation of η_W(%) against immersion time using 4 mM SDS with 500 ppm Zein, it is seen that maximum inhibition efficiency is achieved within 6h of exposure (inset of Fig. 6) and the inhibitor system exhibits appreciable corrosion inhibition property for nearly 48h.

Surface analysis

Scanning electron micrographs (SEM) of the surface of mild steel immersed in 0.5 M H$_2$SO$_4$ solution without and with the inhibitors are shown in Fig. 7 (a,b). With 4 mM SDS in acid medium, mild steel surface shows a very rough surface (Fig. 7a) similar to that observed for blank solution, indicating very low corrosion inhibition potentiality of SDS for the present system. In presence of 4 mM SDS together with 500 ppm Zein, a cleaner and smoother metal surface can be observed (Fig. 7b). This shows the efficacy of Zein-SDS complex system as corrosion inhibitor for mild steel in H$_2$SO$_4$ solution.

RSC Advances Accepted Manuscript
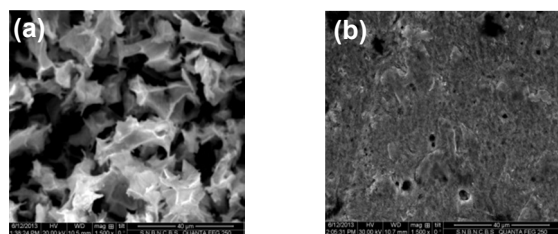
Fig. 7 SEM images of mild steel after immersion in 0.5 M H$_2$SO$_4$ having (a) only SDS (b) SDS with Zein.

In order to determine the functional groups responsible for binding on metal surface, we have examined and compared the FTIR spectra of native Zein, native SDS, surface adsorbed SDS and surface adsorbed Zein-SDS system (fig. 8a-d). Among various bands observed for native Zein sample, main bands are amide I (mainly stretching vibration of C=O group, 1657 cm^{-1}), amide II (in-plane N-H bending, 1532 cm^{-1}), deformation vibration of C-H from CH$_2$ of protein (1444 cm^{-1}). Bands in the range of 2920 cm^{-1} to 2850 cm^{-1} are due to aliphatic C-H stretching vibrations.[18,32-33] SDS, on the other hand, shows its characteristic bands at (Fig. 8b) 1472 cm^{-1} (bending mode of CH$_2$-), doublet at 1254 and 1218 cm^{-1} (asymmetric S-O stretching), 1080 cm^{-1} (symmetric S-O stretching).[34] In case of surface adsorbed SDS (Fig. 8c), all these bands are observed with much lower intensity and shifted towards low wavenumber region (1080 cm^{-1} band shifts at 1017 cm^{-1}). This clearly suggests that SDS adsorbs on mild steel surface through anionic head group (i.e. –O-SO$_3^-$), which is also reported by others.[21,29] In surface adsorbed Zein-SDS aggregate, amide I band of Zein is seen to give a prominent red shift at 1636 cm^{-1} (Fig. 8d). Any possible shifts of other bands are too weak to resolve. Thus it may be concluded that head groups of SDS micelle and amide linkages present in protein chain are mostly responsible for adsorption of Zein-SDS aggregate on the metal surface.
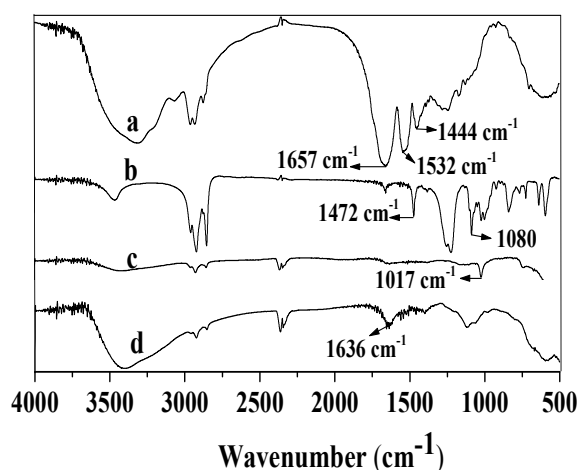
Fig. 8. FTIR spectra of (a) native Zein, (b) native SDS, (c) surface adsorbed SDS, and (d) surface adsorbed Zein-SDS.

Discussion

Novelty of the work lies in the fact that as Zein is insoluble in aqueous solution, and SDS with concentration of 2 mM and higher does not show any significant corrosion inhibition for mild steel in H$_2$SO$_4$ solution, thus the profound corrosion inhibitory action observed for Zein in presence of SDS is mostly due to the effect of
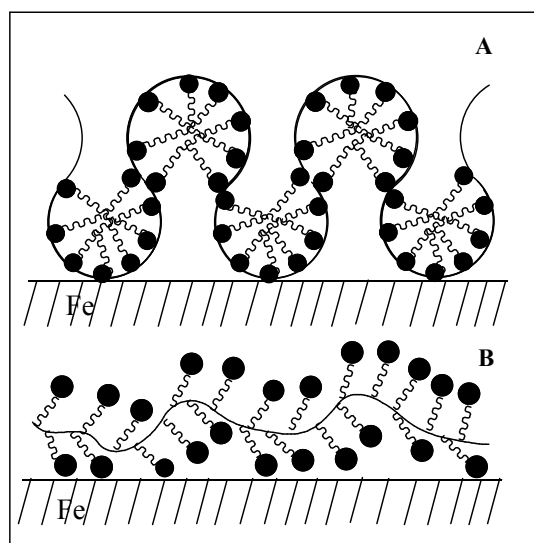
Scheme 1 SDS dependent conformational change of Zein and possible mode of adsorption of Zein-SDS system on mild steel surface.

protein-surfactant aggregate (Scheme 1). From the electrochemical measurements it is observed that SDS micelles at a concentration range much higher than its CMC, adsorb on the mild steel surface in acid medium to a small extent and cannot

alter the rate of either the cathodic reduction reaction or anodic metal dissolution reaction significantly. This may be attributed to possible electrostatic repulsion between the positively charged metal surfaces with large number of Na^+ counter ions associated with of SDS micelles at high concentration. But, for Zein-SDS aggregate, which is seen to behave as mixed type inhibitor, we can find substantial increase in inhibition efficiency. It is reported that when a polymer wraps the micelles forming polymer-surfactant aggregate (Necklace-bead model, Scheme 1A), some of the counter ions as well as water molecules are replaced from the Stern layer of the micelle, and it makes the Stern layer more hydrophobic.[35] Thus, in Zein-SDS aggregate, SDS micelles have more affinity for adoption on steel surface, than that for bare SDS micelles. Also, Zein itself has the amide linkages in its backbone chain, which also get involved in adsorption on metal surface through the lone pairs present on O and N heteroatoms. It may thus be presumed that in case of protein-surfactant aggregate, both the protein and micelle cooperatively or synergistically influence each other in the overall adsorption process. Such cooperative interaction between a polymer or polysaccharide (a biopolymer) with surfactant towards inhibition of corrosion is already reported.[36,37]

The observation that when surfactant-protein ratio increases, inhibition efficiency begins to fall, may be interpreted in terms of surfactant induced conformational change of protein. Zein, itself is insoluble in aqueous medium due to its globular structure. With gradual increase in concentration of SDS, polymer-surfactant aggregate (Necklace-bead model, Scheme 1A) forms and Zein becomes soluble. Formation of such aggregate is initiated from the electrostatic attraction between the partial positive charge of Zein and negatively charged polar head groups of SDS micelles.[19,20] This aggregated state is mostly responsible for showing high inhibition efficiency (Scheme 1A), as discussed above. For further increase in SDS concentration, when all the positive charge of Zein is neutralized, hydrophobic SDS chain interacts with hydrophobic backbone of protein and thus Zein becomes completely unfolded and surrounded by SDS molecules.[19,20] It gradually hinders the direct interaction between Zein molecules and mild steel surface (Scheme 1B). At this stage, mostly the cathodic sites on the metal surface become exposed to the acid solution (may be due to electrostatic repulsion between negatively charged cathodic sites and negatively charged surfactant head

groups), thereby enhancing the rate of cathodic reduction reaction, and hence, overall rate of corrosion.

Conclusions

SDS with concentration much higher than its CMC, does not show any appreciable effect on rate of corrosion of mild steel in 0.5M H_2SO_4 solution. When water insoluble Zein is added in SDS micellar system, soluble Zein-SDS aggregate is formed, which is initiated by electrostatic attraction and subsequent wrapping of the micellar surface by protein chain (necklace-bead model). Zein-SDS aggregate shows strong affinity for adsorption on the mild steel surface thereby enhancing the resistance towards charge transfer reactions occurring there. Zein-SDS aggregate acts as mixed type corrosion inhibitor decreasing the rate of both cathodic and anodic reactions. While SDS is adsorbed on mild steel surface through the $-O-SO_3^-$ group, Zein uses mostly the amide linkages present in its chain for such purpose. Extent of corrosion inhibition is seen to depend on the surfactant-protein ratio, as observed from adsorption isotherm studies. This has been explained in terms of SDS induced conformational change of Zein.

References

1   P.B. Raja, M.G. Sethuraman, Mater. Lett., 2008, **62**, 113.

2   G. Gece, Corros. Sci., 2011, **53**, 3873.

3   S. Shen, C. Zhu, X. Guo, C. Li, Y. Wen, H. Yang, RSC Adv., 2014, **4**, 10597.

4   S.A. Umoren, The Open Corros. J., 2009, **2**, 175.

5   C. Dagbert, T. Meylheuc, M.–N. Bellon-Fontaine, Electrochim. Acta, 2006, **51**, 5221.

6   I. Frateur, L. Lartundo-Rojas, C. Méthivier, A. Galtayries, P. Marcus, Electrochim. Acta, 2006, **51**, 1550.

7   F. Zhang, J. Pan, P.M. Claesson, Electrochim. Acta 2011, **56**, 1636.

8   S.A. Umoren, I.B. Obot, E.E. Ebenso, P.C. Okafor, O. Ogbobe, E.E. Oguzie, Anti-Corros. Meth. Mat., 2006, **53**, 277.

9   M.A. Abu-Dalo, A.A.Othman, N.A.F. Al-Rawashdeh, Int. J. Electrochem. Sci., 2012, **7**, 9303.

10 P. Roy, P. Karfa, U. Adhikari, D. Sukul, Corros. Sci., 2014, **88**, 246.

11 S. Cheng, S. Chen, Tao Liu, X. Chang, Y. Yin, Mater. Lett., 2007, **61**, 3276.

12 P.B. Raja, A.K. Qureshi, A.A. Rahim, H. Osman, K. Awang, Corros. Sci., 2013, **69**, 292.

13 P. Roy, A. Pal, D. Sukul, RSC Adv., 2014, **4**, 10607.

14 P. Mourya, S. Banerjee, M.M. Singh, Corros. Sci., 2014, **85**, 352.

15 J.W. Lawton, Cereal Chem., 2002, **79**, 1.

16 R. Shukla, M. Cheryan, Ind. Crop. Prod., 2001, **13**, 171.

17 P. Argos, K. Pedersen, M.D. Marks, B.A. Larkins, J. Biol. Chem., 1982, **257**, 9984.

18 B. Zhang, Y. Luo, Q. Wang, Food Chem., 2011, **124**, 210.

19 N. Deo, S. Jockusch, N. J. Turro, P. Somasundaran, Langmuir, 2003, **19**, 5083.

20 J.M. Ruso, N. Deo, P. Somasundaran, Langmuir, 2004, **20**, 8988.

21 M.A. Malik, M.A. Hashim, F. Nabi, S. A. Al-Thabaiti, Z. Khan, Int. J. Electrochem. Sci., 2011, **6**, 1927.

22 R. Guo, T. Liu, X. Wei, Colloid Surf. A, 2002, **209**, 37.

23 A. Chatterjee, S.P. Moulik, S.K. Sanyal, B.K. Mishra, P.M. Puri, J. Phys. Chem. B, 2001, **105**, 12823.

24 T. Pajkossy, Solid State Ionics, 2005, **176**, 1997.

25 U. Rammelt, G. Reinhard, Corros. Sci., 1987, **27**, 373.

26 J.-B. Jorcin, M.E. Orazem, N. P´eb`ere, B. Tribollet, Electrochim. Acta, 2006, **51**, 1473.

27 X. Wu, H. Ma, S. Chen, Z. Xu, A. Sui, J. Electrochem. Soc., 1999, **146**, 1847.

28 M. Lebrini, F. Robert, C. Roos, Int. J. Electrochem. Sci., 2010, **5**, 1698.

29 R. Fuchs-Godec, V. Doleček, Colloid Surf. A, 2004, **244**, 73.

30 I.L. Rozenfeld, Corrosion Inhibitors, McGreaw-Hill Inc, New York, 1981.

31 K.Y. Foo, B.H. Hameed, Chem. Engg. J., 2010, **156,** 2.

32 T.C. Bicudo, L.A. Forato, L.A.R. Batista, L.A. Colnago, Anal. Bioanal. Chem., 2005, **383**, 291.

33 B. Zhang, Y. Luo, Q. Wang, Biomacromol., 2010, **11**, 2366.

34 R.B. Viana, A.B.F. da Silva, A.S. Pimentel, Adv. Phys. Chem., Article ID 903272, 2012, 14 pages.

35 D. Sukul, S.K. Pal, D. Mandal, S. Sen, K. Bhattacharyya, J. Phys. Chem. B, 2000, **104**, 6128.

36 M.A. Deyab, S.S. Abd El-Rehim, S.T. Keera, Colloid Surf. A, 2009, **348**, 170.

37 M. Mobin, M. A. Khan, M. Parveen, J. Appl. Poly. Sci., 2011, **121**, 1558.